AIP | Applied Physics Letters

Polarization insensitive and omnidirectional broadband near perfect planar metamaterial absorber in the near infrared regime

Shuqi Chen, Hua Cheng, Haifang Yang, Junjie Li, Xiaoyang Duan et al.

Citation: Appl. Phys. Lett. **99**, 253104 (2011); doi: 10.1063/1.3670333
View online: http://dx.doi.org/10.1063/1.3670333
View Table of Contents: http://apl.aip.org/resource/1/APPLAB/v99/i25
Published by the American Institute of Physics.

Polarization insensitive and omnidirectional broadband near perfect planar metamaterial absorber in the near infrared regime

Shuqi Chen,[1] Hua Cheng,[1] Haifang Yang,[2] Junjie Li,[2] Xiaoyang Duan,[1] Changzhi Gu,[2] and Jianguo Tian[1,a)]

[1]*The Key Laboratory of Weak-Light Nonlinear Photonics, Ministry of Education, Teda Applied Physics School and School of Physics, Nankai University, Tianjin 300457, China*

[2]*Beijing National Laboratory for Condensed Matter Physics, Institute of Physics, Chinese Academy of Sciences, P.O. Box 603, Beijing 100190, China*

(Received 1 October 2011; accepted 15 November 2011; published online 21 December 2011)

We present the design, characterization, and experimental demonstration of a polarization insensitive and omnidirectional broadband near perfect planar metamaterial absorber (MA) in the near infrared regime, which does not need to stack multilayer composite structures. Experimental result shows that greater than 80% absorption is obtained across a wavelength range of 0.41 μm, which is in reasonable agreement with the simulation. The electromagnetic response of the MA is theoretically investigated. The broadband planar MA is polarization insensitive and the absorption remains high even at large incident angles. © *2011 American Institute of Physics*. [doi:10.1063/1.3670333]

Since perfect metamaterial absorber (MA) at microwave frequency was demonstrated by Landy *et al.*,[1] research into this topic has grown rapidly.[2,3] Later, many efforts have focused on this perfect MA to achieve polarization insensitive absorption[4,5] or wide angle absorption.[6,7] However, most of these designs are based on strong electromagnetic resonances to effectively absorb the incident light. Consequently, the bandwidth of these perfect MAs is often narrow, which limits the device applications of these absorbing structures. Recently, Wakatsuchi *et al.* demonstrated that highly customizable broadband absorption for arbitrary polarization is possible in the gigahertz regime by use of conductively lossy cut wires (CWs) as MA.[8] Ye *et al.*[9] and Grant *et al.*[10] also proposed a design by stacking multilayer composite structures with different geometrical dimensions, which can be used as a polarization insensitive broadband near perfect MA in the terahertz range. However, the designs in Refs. 8–10 need to precisely align between the layers or stack several composite structures, which complicate the fabrication process. If we want to obtain more broadband MA, more composite structures need to be stacked, so the fabrication of such broadband MA is far complicated and inaccurate than that of planar MA.

In this letter, we present the design, characterization, and experimental demonstration of a broadband near perfect planar MA in the near infrared regime composed of gold CWs, a dielectric spacer and a gold plane layer, which does not need to precisely align between the layers or stack several composite structures. The bandwidth of absorption spectrum can be effectively expanded by hybridizing the electric dipoles of the CWs. The broadband planar MA is polarization insensitive and the absorption remains high even at large incident angles for both transverse electric (TE) and transverse magnetic (TM) configurations, which provide more efficient absorption for the nonpolarized and wide angle incident beams.

a)Author to whom correspondence should be addressed. Electronic mail: jjtian@nankai.edu.cn.

The designed and fabricated broadband planar MA is shown in Fig. 1. It contains two metallic elements: an array of 0.06 μm thick gold structures and a 0.1 μm thick gold board, which are separated by 0.185 μm thick Al_2O_3 with dielectric constant and loss tangent as 2.28 and 0.04.[11] All the three layers are fabricated on silicon substrate with permittivity of 11.7. The optical constants of bulk gold in the infrared spectral regime are described by the Drude model with the plasma frequency $\omega_p = 1.37 \times 10^{16} s^{-1}$ and the damping constant $\omega_c = 4.08 \times 10^{13} s^{-1}$.[12] To more clearly understand the effect of the CWs, we split the double layer CWs into outer layer and inner layer CWs.

The optimized broadband planar MA structure was obtained by using the finite element method based commercial software COMSOL Multiphysics 3.4.[13] We consider a single unit cell with periodic boundary conditions in x and y planes, and waveguide ports boundary conditions on the other boundaries.

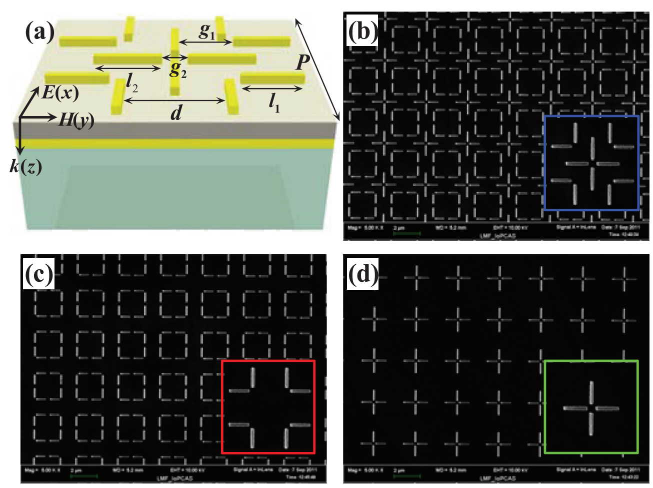

FIG. 1. (Color online) (a) Schematic of the broadband planar MA. The geometry parameters are as: the repeat period p of 3.2 μm, the outer and inner layer CW length of $l_1 = 0.7\,\mu$m and $l_2 = 0.78\,\mu$m, the CW width of $w = 0.12\,\mu$m, and dimensions $g_1 = 0.665\,\mu$m, $g_2 = 0.3\,\mu$m and $d = 1.08\,\mu$m. Top-view SEM images for (b) double layer, (c) outer layer and (d) inner layer structures, respectively. Inset: Enlarged view.

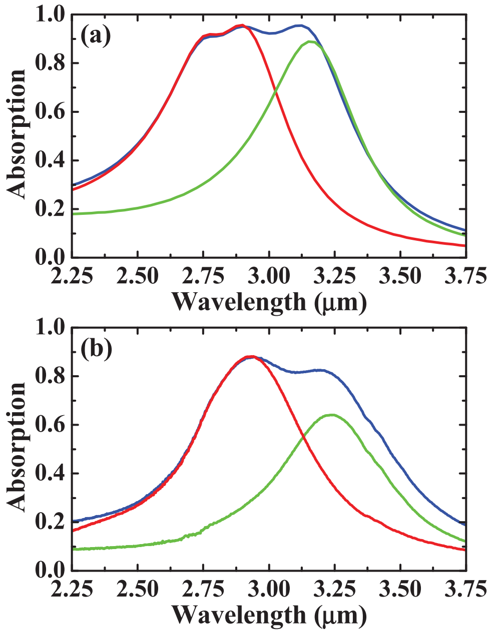

FIG. 2. (Color online) (a) Simulated and (b) experimental absorption spectra of outer layer (red line), inner layer (green line), and double layer (blue line) structures for normal incidence.

As the thickness of the ground plane is much larger than the typical skin depth in the near infrared regime, the absorption can be calculated using $A(\omega) = 1 - R(\omega)$. Considering an incident beam normal incidence to the MA, the simulated absorption spectra as a function of wavelength for three optimized structures are shown in Fig. 2(a). Two metallic elements with CWs and a ground plane often show single band perfect MA in infrared regime.[11] However, by introducing outer layer CWs with a fourfold rotational symmetry, the bandwidth of absorption spectrum can be effectively expanded. The absorption peaks of two resonances at 2.78 μm and 2.90 μm are 92% and 96%, respectively. The structure with inner layer CWs exhibits a single resonant peak at 3.15 μm with 89% absorption. When the two separated structures are combined together, the resonant peaks of the two separated structures are merged in the absorption spectrum due to the hybridization of the electric dipoles. The resonant absorption of 91%, 95% and 96% can be obtained for three resonant peaks 2.78 μm, 2.90 μm, and 3.13 μm, respectively. The bandwidth with absorption greater than 90% is 0.44 μm.

Standard E-beam deposition and E-beam lithography techniques were used to fabricate the MA. First, a Ti (5 nm)/Au (100 nm) metallic ground pane were deposited on a 3 mm thick silicon substrate by E-beam deposition. This was followed by E-beam deposition of a 185 nm thick layer of Al_2O_3. The top patterned layer was defined by the E-beam lithography. Then Cr (5 nm)/Au (60 nm) were evaporated, and the pattern transfer was completed by metal liftoff. Figure 1 shows the scanning electron microscopy (SEM) image of the fabricated MA. Bruker VERTEX 70 Fourier-transform IR spectrometer was used to measure the reflection spectrum. The reflection of the sample was recorded by averaging measured data over 64 measurements in order to improve the signal-to-noise ratio. For reflection measurements, the incident unpolarized light was inclined with an angle of about 30° with respect to the normal on the sample surface. Before measuring the MA sample, the reflection was calibrated with a gold plate. The experimentally obtained absorption spectra of three designed structures are shown in Fig. 2(b). An apparent broadband absorption is obtained, which is in reasonable agreement with the simulated result. The bandwidth with absorption greater than 80% is 0.41 μm. There is a redshift of 0.09 μm between experimental and simulated results due to the inaccuracy of the fabricated CW length. As the left resonance is very sensitive to the outer layer CW length, the left resonant absorption peak is unapparent, which is merged with middle absorption peak.

To better understand the nature of this broadband planar MA, we investigated the surface current and electric field distribution through numerical simulation. The surface current distribution and the electric field modulus in the surface of the gold CWs at three absorption peaks are shown by red arrows and colormaps in Figs. 3(a), 3(c), and 3(e), respectively. Meanwhile, the surface current distributions in the ground gold plane are also shown in Figs. 3(b), 3(d), and 3(f). For the left resonance, the surface currents are noticeably distributed in the horizontal gold CWs of the outer layer and the electric field is strongly enhanced at the end of these CWs. Strong electric dipole resonances exist in these CWs resulting from charges accumulated at two sides of gold

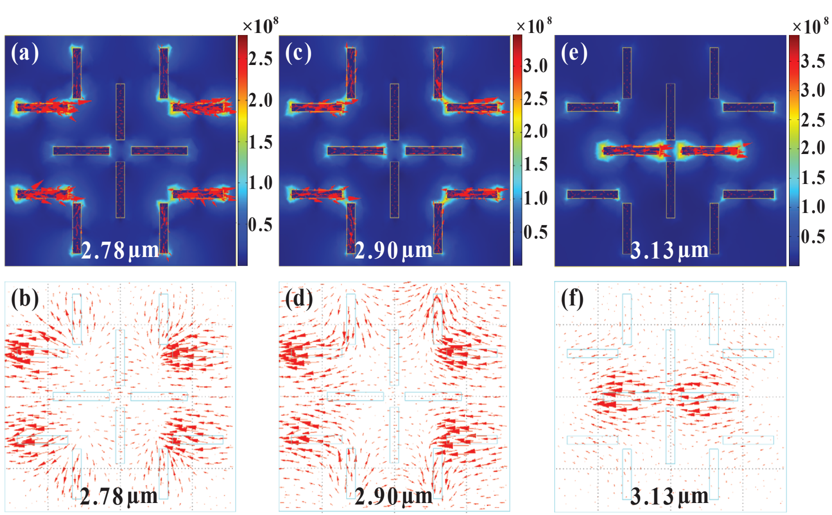

FIG. 3. (Color online) The surface current distribution (red arrows) and the electric field modulus (colormaps) in the surface of the gold CWs at the wavelengths of (a) 2.78 μm, (c) 2.90 μm, and (e) 3.13 μm. The surface current distribution (red arrows) in the ground gold plane corresponding to the wavelengths of (b) 2.78 μm, (d) 2.90 μm, and (f) 3.13 μm.

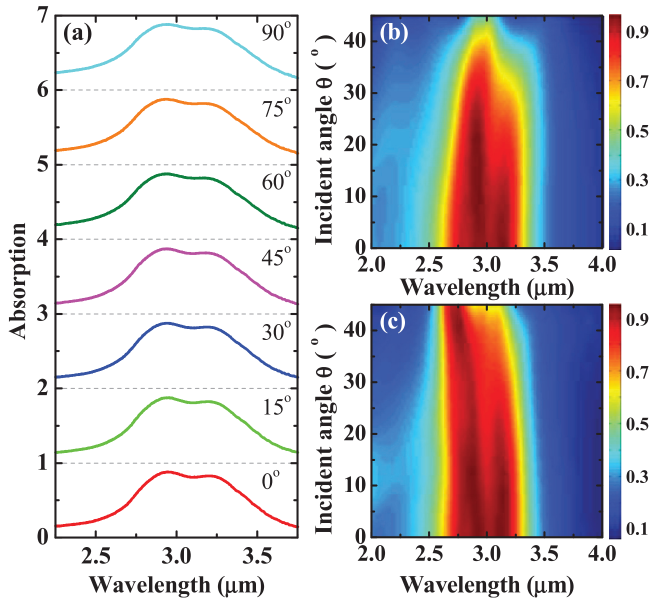

FIG. 4. (Color online) (a) Experimental absorption spectra of composite structure for different incident polarizations. Simulated angular dispersion of the absorption spectra for both (b) TE and (c) TM configurations, respectively.

CWs. For the middle resonance, the surface currents are distributed in the horizontal and vertical gold CWs of the outer layer, thus the electric dipole resonances are excited in two adjacent gold CWs. For the right resonance, the absorption effect is due to the excitation of localized electric dipole resonances in the horizontal gold CWs of the inner layer. Therefore, the resonant peaks in both outer layers and inner layers are merged in the absorption spectrum and forming a broadband near perfect MA as the hybridization of the electric dipoles between two layers. In addition, the surface currents in the top gold CWs and the ground gold plane are opposite to each other. The magnetic field accumulates in the dielectric spacer between them. Magnetic dipole resonances are also contributed to the absorption effect.

The polarization insensitive performance is important in practical applications. In some cases, most of possible light needs to be absorbed, which may contain arbitrarily polarized components. To demonstrate the polarization insensitive behavior, we placed a near infrared polarizer in the beam path so that the incident beam was linearly polarized. The experimental absorption spectra of the composite structure for different incident polarizations are shown in Fig. 4(a). Results show that the absorption spectra of the fabricated broadband planar MA are polarization insensitive. Our designed broadband structure can also work as near perfect MA over a wide range of incident angles θ. Figures 4(b) and 4(c) give the simulated angular dispersion of the absorption spectra for both TE and TM configurations, respectively. For the TE case, the broadband absorption characteristics can be maintained with the increasing the incident angle. However, when the incident angle is beyond 45°, there is a monotonic decrease in the absorption and bandwidth. With the increasing of the incident angle, the incident magnetic field between the two metallic layers becomes less and less, which can no longer efficiently drive a strong magnetic resonance. For the case of TM polarization, the broadband absorption characteristics are nearly independent of incident angle. The absorption decreases slightly and the bandwidth narrows gradually when the incident angles vary from 60° to 80°. In this case, the magnetic field can effectively provide the strong magnetic resonance at all incident angles. These simulated results reveal that the proposed broadband planar MA operates quite well for both TE and TM radiation over a wide range of incident angles.

In conclusion, we have designed and fabricated a polarization insensitive and omnidirectional broadband near perfect planar MA in the near infrared regime constructed with gold CWs, a dielectric spacer and a gold plane layer. The bandwidth of absorption spectrum can be effectively expanded by hybridizing the electric dipoles of CWs. It can be expected that not restricted to two layers but more layers of CWs can be introduced to obtain a wider bandwidth of near perfect MA. The proposed broadband near perfect MA does not need to well align between the layers or stack several composite structures, which simplifies the fabrication process. It may find numerous applications ranging from a thermal detector to a coating material to mitigate spurious reflections.

This research was supported by the Chinese National Key Basic Research Special Fund (Grant No. 2011CB922003), National Natural Science Foundation of China (Grant Nos. 61008002, 50825206, and 91023041), the Specialized Research Fund for the Doctoral Program of Higher Education (Grant No. 20100031120005), the Fundamental Research Funds for the Central Universities (Grant Nos. 65010801 and 65012351), the Knowledge Innovation Project of CAS (Grant No. KJCX2-EW-W02), and 111 project (Grant No. B07013).

[1]N. I. Landy, S. Sajuyigbe, J. J. Mock, D. R. Smith, and W. J. Padilla, Phys. Rev. Lett. **100**, 207402 (2008).
[2]J. Hao, J. Wang, X. Liu, W. J. Padilla, L. Zhou, and M. Qiu, Appl. Phys. Lett. **96**, 251104 (2010).
[3]J. A. Mason, S. Smith, and D. Wasserman, Appl. Phys. Lett. **98**, 241105 (2011).
[4]N. I. Landy, C. M. Bingham, T. Tyler, N. Jokerst, and D. R. Smith, and W. J. Padilla, Phys. Rev. B **79**, 125104 (2009).
[5]Y. Ma, Q. Chen, J. Grant, S. C. Saha, A. Khalid, and D. R. S. Cumming, Opt. Lett. **36**, 945 (2011).
[6]H. Tao, C. M. Bingham, A. C. Strikwerda, D. Pilon, D. Shrekenhamer, N. I. Landy, K. Fan, X. Zhang, W. J. Padilla, and R. D. Averitt, Phys. Rev. B **78**, 241103 (2008).
[7]Y. Avitzour, Y. A. Urzhumov, and G. Shvets, Phys. Rev. B **79**, 045131 (2009).
[8]H. Wakatsuchi, S. Greedy, C. Christopoulos, and J. Paul, Opt. Express **18**, 22187 (2010).
[9]Y. Q. Ye, Y. Jin, and S. He, J. Opt. Soc. Am. B **27**, 498 (2010).
[10]J. Grant, Y. Ma, S. Saha, A. Khalid, and D. R. S. Cumming, Opt. Lett. **36**, 3476 (2011).
[11]X. Liu, T. Starr, A. F. Starr, and W. J. Padilla, Phys. Rev. Lett. **104**, 207403 (2010).
[12]M. A. Ordal, L. L. Long, R. J. Bell, S. E. Bell, R. R. Bell, R. W. Alexander, and C. A. Ward, Appl. Opt. **22**, 1099 (1983).
[13]COMSOL Multiphysics User's Guide, Version 3.4, Comsol AB, Burlington, Mass (2008).